INTERNATIONAL JOURNAL OF
NUMERICAL ANALYSIS AND MODELING
Volume 20, Number 1, Pages 134–151

© 2023 Institute for Scientific
Computing and Information
doi: 10.4208/ijnam2023-1006

THE MIXED FINITE VOLUME METHODS FOR STOKES PROBLEM BASED ON MINI ELEMENT PAIR

HONGTAO YANG AND YONGHAI LI*

Abstract. In this paper, we present and analyze MINI Mixed finite volume element methods (MINI-FVEM) for Stokes problem on triangular meshes. The trial spaces for velocity and pressure are chosen as MINI element pair, and the test spaces for velocity and pressure are taken as the piecewise constant function spaces on the respective dual grid. It is worth noting that the bilinear form derived from the gradient operator and the bilinear form derived from the divergence are unsymmetric. With the help of two new transformation operators, we establish the equivalence of bilinear forms for gradient operator between finite volume methods and finite element methods, and the equivalence of bilinear forms for divergence operator between finite volume methods and finite element methods, so the inf-sup conditions are obtained. By the element analysis methods, we give the positive definiteness of bilinear form for Laplacian operator. Based on the stability, convergence analysis of schemes are established. Numerical experiments are presented to illustrate the theoretical results.

Key words. Stokes problem, MINI element, mixed finite volume methods, inf-sup condition.

1. Introduction

The Stokes problem, as a basic problem in incompressible fluid mechanics and a classical prototype model of mixed problems, has been extensively studied. There are many research about finite element methods(MFEM), for which reader is referred to [19, 6, 7, 3, 28] and the references cited therein. The MFEM theory [4] shows that an elementary requirement, which makes discretization system corresponding to Stokes problems, is that the velocity-pressure element pair satifies the inf-sup condition. For solving the Stokes problem, there are many velocity-pressure element pairs to be constructed[1, 6], and many stabilization technology is proposed[5, 20]. The finite volume method is also a common numerical method for partial differential equations. Due to the local conservation property, fintie volume method is widely used in computational fluid dynamic[27, 16, 17, 2, 31, 18].

Finite volume element method(FVEM), which belongs to a kind of Petrov-Galerkin methods, is an important type of finite volume method. By choosing the Lagrange type finite element space as the trial space and using the piece constant function space on the dual grid as the test space, a complete theoretical framework of FVEM is established like finite element methods[27, 9, 42, 29, 37]. There are many scholars studied finite volume methods for Stokes problem. The finite volume methods by using the nonconforming elements space for velocity and the piecewise constants for pressure is studied in [11, 13, 39]. The finite volume methods by using the conforming elements space for velocity and the piecewise constants for pressure is studied in [12, 33, 41, 40]. Ye in paper [38] investigate the relatonshape between finie volume and finite element both conforming and unconforming velocity space and constants pressure space. The unified analysis and error estimation is established in [15, 26, 8]. For research on the finite volume method

Received by the editors on April 1, 2022 and, accepted on October 15, 2022.
2000 *Mathematics Subject Classification.* 65N08, 76D07, 76M12.
*Corresponding author.

whose velocity and pressure are both conforming elements space, they either use stablilized equal order pairs[22, 21, 32, 36], or discrete continuity equations by finte element methods[22, 32, 10]. MAC-like(Marker-And-Cell) finite volume methods on staggered grids are studied in the papers [12, 30, 35]. As the same time, scholars also extended the finite volume method to the Navier-Stokes equations[25, 23, 24] and other complex fluid problems[34].

In this article, we construct and analyze the MINI mixed finite volume element methods for Stokes problem. Based on the primary trianguler meshes, two different dual meshes associated with velocity and pressure are constructed. Then, the trial space for velocity and pressure are taken as MINI element pair, and the test spaces for velocity and pressure are choosen as the piecewise constants space on respective dual meshes. So we construct a full finite volume scheme for both momentum equation and continuity equation. Obviously, the schemes satisfy the local conservation of mass on dual element of pressure. However, the bilinear form derived from the gradient operator and the bilinear form derived from the divergence are unsymmetric, and they are all different from the corresponding bilinear form in mixed finite element methods. With the help of two new transformation operators, we establish the equivalence of bilinear forms for gradient operator between FVEM and MFEM, and the equivalence of bilinear forms for divergence operator between FVEM and MFEM, then the inf-sup conditions are obtained. Moreover, the equivalence of bilinear forms for gradient operator and divergence operator is obtained. The stability of bilinear form for Laplacian operator is proved by the element analysis methods. Based on the stability of saddle point system, the error estimations are proved.

The outline of the this paper is as follows. In section 2, we construct the MINI mixed finite volume methods for Stokes problem. In section 3, the continuity and stability of the bilinear forms are establish. We carry out the convergence analysis for the MINI mixed finite volume methods in section 4. In section 5, numerical experiments are presented to confirm the theoretical result.

2. The MINI mixed finite volume element methods

In this section, we establish the MINI mixed finite volume method for the Stokes equations

$$\left\{\begin{array}{rcll} -\nu\Delta\boldsymbol{u}+\nabla p &=& \boldsymbol{f}, & \text{in } \Omega, \\ \operatorname{div}(\boldsymbol{u}) &=& 0, & \text{in } \Omega, \\ \boldsymbol{u} &=& \boldsymbol{0}, & \text{on } \partial\Omega, \end{array}\right. \tag{1}$$

where Ω is a bounded polyhedral domain in $\mathbb{R}^2$, $\nu > 0$ is the kinematic viscosity, $\boldsymbol{u} = (u^x, u^y)$ is the fluid velocity, p is the pressure and $\boldsymbol{f} = (f^x, f^y)$ is the give body force per unit mass. For a non-negative integer k and $\mathcal{D} \in \mathbb{R}^2$, let $H^k(\mathcal{D})$ denote the Sobolev space with the norm $\|\cdot\|_{k,\mathcal{D}}$ and the semi-norm $|\cdot|_{k,\mathcal{D}}$. When $\mathcal{D} = \Omega$, we take $|\cdot|_k$ denote $\|\cdot\|_{k,\Omega}$. Then, we introduce the following spaces

$$L_0^2(\Omega) := \left\{p \in L^2(\Omega) : \iint_\Omega p dxdy = 0\right\}, \tag{2}$$

$$H_0^1(\Omega) := \left\{v \in H^1(\Omega) : v|_{\partial\Omega} = 0\right\}. \tag{3}$$

Furthermore, the variational problem corresponding to the equation (1) can be expressed as finding $(\boldsymbol{u}, p) \in \left(H_0^1(\Omega)\right)^2 \times L_0^2(\Omega)$, such that

$$\left\{ \begin{array}{rcll} a(\boldsymbol{u},\boldsymbol{v}) - b(\boldsymbol{v},p) & = & \langle \boldsymbol{f}, \boldsymbol{v}\rangle, & \forall \boldsymbol{v} \in \left(H_0^1(\Omega)\right)^2, \\ b(\boldsymbol{u},q) & = & 0, & \forall q \in L_0^2(\Omega), \end{array} \right. \tag{4}$$

where

$$a(\boldsymbol{u},\boldsymbol{v}) = \nu \iint_\Omega \nabla \boldsymbol{u} : \nabla \boldsymbol{v} dxdy, \tag{5}$$

$$b(\boldsymbol{u},q) = \iint_\Omega q \operatorname{div}(\boldsymbol{u}) dxdy. \tag{6}$$

2.1. Primary meshes and trial space. Let $\mathcal{T}_h = \{K\}$ be a quasi-uniform triangular partition of Ω, which means there exist constant σ such that

$$min\{\rho_K, K \in \mathcal{T}_h\} \geq \sigma h, \tag{7}$$

where ρ_K largest circle contained in K, and $h = \max h_K$, here h_K is the diamerter of element K. We denote by $\mathcal{P}_h$ the set of all vertices of triangular elements, and by $\mathcal{O}_h$ the set of all barycenters of triangular elements. And we define $H_h^k(\Omega) = \{v \in L^2(\Omega) : v|_K \in H^k(K), \forall K \in \mathcal{T}_h\}$.

we define $\mathbb{P}_1$ denote the linear polynomials space, and $\mathbb{P}_{1+b}$ denote the linear polynomials space enriched with bubble functions. Then any $v \in \mathbb{P}_1(K)$ can be written as

$$v(\lambda_1, \lambda_2, \lambda_3) = v_1\lambda_1 + v_2\lambda_2 + v_3\lambda_3, \tag{8}$$

and $v \in \mathbb{P}_{1+b}(K)$ can be written as

$$v(\lambda_1, \lambda_2, \lambda_3) = v_1\lambda_1 + v_2\lambda_2 + v_3\lambda_3 + 27v_b\lambda_1\lambda_2\lambda_3, \tag{9}$$

where $v_b = v_0 - \frac{1}{3}(v_1 + v_2 + v_3)$, v_0 and $v_i (i = 1, 2, 3)$ represent the value of v at the barycenter and the vertices respectively, and $\lambda_i, i = 1, 2, 3$ denote the area coordinates.

We take the MINI mixed finite elements space pair $[\mathbb{P}_{1+b}]^2/\mathbb{P}_1$ as the trial spaces of velocity and pressure respectively, which is a stable Stokes pair from mixed finite element methods[1].

The trial function space for velocity component is taken as

$$V_h = \{u_h \in C(\Omega) : u_h|_K \in \mathbb{P}_{1+b}(K), \forall K \in \mathcal{T}_h, u_h|_{\partial\Omega} = 0\}, \tag{10}$$

we can split any $u_h \in V_h$ as

$$u_h = u_h^l + u_h^b, \tag{11}$$

where u_h^l is the linear part and the u_h^b is the bubble part.

The trial space for pressure is taken as

$$Q_h = \left\{p_h \in L_0^2(\Omega) : p_h \in \mathbb{P}_1(K), \forall K \in \mathcal{T}_h\right\}. \tag{12}$$

In the paper [1], D. N. Arnold et al. prove that $[\mathbb{P}_{1+b}]^2/\mathbb{P}_1$ pair satifies discrete inf-sup condition

$$\sup_{\boldsymbol{v}_h \in (V_h)^2 \setminus \{\boldsymbol{0}\}} \frac{b(\boldsymbol{v}_h, q_h)}{|\boldsymbol{v}_h|_1} \geq \gamma_0 \|q_h\|_0. \tag{13}$$

2.2. Dual meshes and test space. Since the distribution of interpolation nodes in velocity space is different from in pressure spaces, we need to construct different dual meshes and corresponding test functions space for velocity and pressure respectively.

2.2.1. Dual meshes and test space for velocity. Accroding to the position of interpolation nodes in velocity space, we construct the dual meshes as follow. By connecting the midpoints of any two edges on the triangular element $K \in \mathcal{T}_h$, we divide the each triangle into four sub-triangles corresponding to the vertices and barycenter, see Figure 1(a).

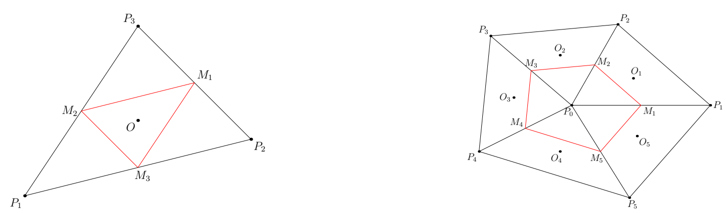

(a) Dual element surrounding barycenter (b) Dual element surrounding vertex

FIGURE 1. Dual element for velocity.

The dual element $K^*_{v,O}$ surrounding the barycenters $O \in \mathcal{O}_h$ is the triangle $\triangle M_1M_2M_3$ see Figure 1(a). The dual element K^*_{v,P_0} associated with P_0 is formed by all sub-triangles with P_0 as the vertex, see Figure 1(b). The dual elements corresponding to all vertices and barycenters constitute the dual parition $\mathcal{T}^*_{h,v} = \{K^*_{v,P},\ K^*_{v,O},\ P \in \mathcal{P}_h,\ O \in \mathcal{O}_h\}$.

The test function space corresponding velocity component space V_h is defined as

$$V_h^* = \left\{ v_h \in L^2(\Omega) : v_h|_{K_v^*} \text{ is constant}, \quad \forall K_v^* \in \mathcal{T}^*_{h,v}, v_h|_{K^*_{v,P}} = 0, \forall P \in \partial\Omega \right\}. \tag{14}$$

2.2.2. Dual meshes and test space for pressure. The dual element for pressure construct as follow. By connecting the barycenter O and the midpoints of three edges of triangular element, we divide the triangular element into three sub-quadrilaterals, see Figure 2(a). Then the dual element surrounding vertex P_0 is formed by all sub-quadrilaterals with P_0 as the vertex, see Figure 2(b). The dual elements corresponding to all vertices constitute the dual parition $\mathcal{T}^*_{h,p} = \{K^*_{p,P},\ P \in \mathcal{P}_h\}$.

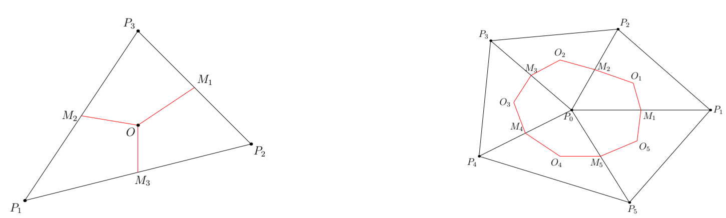

(a) Dual element for pressure on one triangular (b) Dual element surrounding vertex

FIGURE 2. Dual element for pressure.

The test function space corresponding pressure space Q_h is defined as

$$Q_h^* = \left\{ q_h \in L_0^2(\Omega) : q_h|_{K_p^*} \text{ is constant}, \ \forall K_p^* \in \mathcal{T}^*_{h,p} \right\}. \tag{15}$$

2.3. The fintie volume methods. Firstly, we introduce the following bilinear forms and inner product:

$$a_h(\boldsymbol{u}_h,\boldsymbol{v}_h) = -\sum_{K_v^*\in T_{h,v}^*}\int_{\partial K_v^*}\nu\frac{\partial \boldsymbol{u}_h}{\partial \boldsymbol{n}}\cdot\boldsymbol{v}_h ds, \qquad \boldsymbol{u_h}\in(V_h)^2, \boldsymbol{v}_h\in(V_h^*)^2, \tag{16}$$

$$b_h^1(\boldsymbol{v}_h,p_h) = \sum_{K_v^*\in T_{h,v}^*}\int_{\partial K_v^*} p_h\boldsymbol{v}_h\cdot\boldsymbol{n}ds, \qquad \boldsymbol{v}_h\in(V_h^*)^2, p_h\in Q_h, \tag{17}$$

$$b_h^2(\boldsymbol{u}_h,q_h) = \sum_{K_q^*\in T_{h,p}^*}\iint_{K_q^*}\mathrm{div}(\boldsymbol{u}_h)q_h dxdy, \qquad \boldsymbol{u}_h\in(V_h)^2, q_h\in Q_h^*, \tag{18}$$

$$(\boldsymbol{f},\boldsymbol{v}_h) = \sum_{K_v^*\in T_{h,v}^*}\iint_{K_v^*}\boldsymbol{f}\cdot\boldsymbol{v}_h dxdy, \qquad \boldsymbol{v}_h\in(V_h^*)^2, \tag{19}$$

where $\boldsymbol{n}$ denote unit outward normal vector to ∂K_v^*.

The MINI mixed finite volume element method for Stokes problem (1) is to find $(\boldsymbol{u}_h,p_h)\in(V_h)^2\times Q_h$, such that

$$\left\{\begin{array}{rcll} a_h(\boldsymbol{u}_h,\boldsymbol{v}_h)+b_h^1(\boldsymbol{v}_h,p_h) &=& \langle\boldsymbol{f},\boldsymbol{v}_h\rangle, & \forall\boldsymbol{v}_h\in(V_h^*)^2,\\ b_h^2(\boldsymbol{u}_h,q_h) &=& 0, & \forall q_h\in Q_h^*, \end{array}\right. \tag{20}$$

In the following, we introduce two projection operator:
Firstly, we let Π_v^* be the projection operator from V_h to V_h^* as follow

$$\Pi_v^* u_h = \sum_{P\in\mathcal{P}_h\cup\mathcal{O}_h}\left(u_h^l(P)+\frac{11}{4}u_h^b(P)\right)\psi_P^v, \tag{21}$$

here ψ_P^v is the characteristic function defined on dual element $K_{v,P}^*\in\mathcal{T}_{h,v}^*$. the value of $\Pi_v^*u_h$ is equal to $u_h(P)$ on dual element K_P^* corresponding to vertex $P\in\mathcal{P}_h$, and equal to $u_h^l(O)+\frac{11}{4}u_h^b(O)$ on dual element K_O^* corresponding to barycenter $O\in\mathcal{O}_h$. Secondly, let Π_p^* denote the projection operator from Q_h to Q_h^*

$$\Pi_p^* p_h = \sum_{P\in\mathcal{P}_h} p_h(P)\psi_P^p, \tag{22}$$

here ψ_P^p is the characteristic functions defined on dual element $K_{p,P}^*\in\mathcal{T}_{h,p}^*$.

Then the variational equations (20) is equivalent to

$$\left\{\begin{array}{rcll} a_h(\boldsymbol{u}_h,\Pi_v^*\boldsymbol{v}_h)+b_h^1(\Pi_v^*\boldsymbol{v}_h,p_h) &=& \langle\boldsymbol{f},\Pi_v^*\boldsymbol{v}_h\rangle, & \forall\boldsymbol{v}_h\in(V_h)^2,\\ b_h^2(\boldsymbol{u}_h,\Pi_p^*q_h) &=& 0, & \forall q_h\in Q_h. \end{array}\right. \tag{23}$$

3. Stability

In this section, we establish the satility of the MINI mixed finite volume methods. By establishing the equivalence of $b_h^1(\cdot,\cdot)$ and $b(\cdot,\cdot)$, and the equivalence of $b_h^2(\cdot,\cdot)$ and $b(\cdot,\cdot)$, respectively, we prove the Inf-Sup conditions of $b_h^1(\cdot,\cdot)$ and $b_h^2(\cdot,\cdot)$. Firstly, we indroduce the following discrete semi-norms, which play a vital role in stability analysis.

We define the discrete semi-norm $|\cdot|_{1,V_h}$ on trial space V_h, for all $w_h\in V_h$

$$|w_h|_{1,V_h} = \left(\sum_{K\in\mathcal{T}}|w_h|_{1,V_h,K}^2\right)^{1/2}, \tag{24}$$

and

$$|w_h|_{1,V_h,K}^2 = Y_1^2 + Y_2^2 + Y_3^2,$$

where $Y_i = w_h(P_i) - w_h(O)$, here $P_i (i = 1, 2, 3)$ are vertices, and O is the barycenter of triangular element K. And we define the discrete semi-norm $|\cdot|_{1,V_h^*}$ on test space V_h^*, for any $w_h \in V_h^*$

$$|w_h|_{1,V_h^*} = \left(\sum_{E \in \mathcal{E}_{\mathcal{T}_{h,v}^*}} \frac{1}{|E|} \int_E [w_h]^2 \, ds \right)^{1/2}, \tag{25}$$

where $\mathcal{E}_{\mathcal{T}_{h,v}^*}$ denotes the set of boundary segments of all dual elements in $\mathcal{T}_{h,v}^*$, $[w_h] = w_h|_{K_{v,1}^*} - w_h|_{K_{v,2}^*}$ denotes the jump of w_h on edge E, where $K_{v,1}^*$ and $K_{v,2}^*$ are two adjacent dual elements, and $|E|$ is the length of E.

Next, we show that the discrete semi-nomrs $|\cdot|_{1,V_h}$ and $|\Pi_v^* \cdot|_{1,V_h^*}$ and the Sobolev semi-norm $|\cdot|_1$ have the following properties.

Lemma 3.1. *Assume $\mathcal{T}_h$ is regular, then there exist positive constants c_1 and C_1, such that*

$$c_1 |w_h|_{1,V_h} \le |w_h|_1 \le C_1 |w_h|_{1,V_h}, \quad w_h \in V_h, \tag{26}$$

and there exist positive constants c_2 and C_2, such that

$$c_2 |w_h|_{1,V_h} \le |\Pi_v^* w_h|_{1,V_h^*} \le C_2 |w_h|_{1,V_h}, \quad w_h \in V_h. \tag{27}$$

Proof. Since $w_h|_K$ can be expressed in the form (9), and $\lambda_1 + \lambda_2 + \lambda_3 = 1$, we have

$$\begin{aligned} \frac{\partial w_h}{\partial \lambda_2} &= (Y_1 - Y_2) + 9(\lambda_3 - 2\lambda_2\lambda_3 - \lambda_3^2)(Y_1 + Y_2 + Y_3), \\ \frac{\partial w_h}{\partial \lambda_3} &= (Y_1 - Y_3) + 9(\lambda_2 - 2\lambda_2\lambda_3 - \lambda_2^2)(Y_1 + Y_2 + Y_3). \end{aligned} \tag{28}$$

In addition, by the chain rule

(29)

$$\left(\frac{\partial w_h}{\partial x}\right)^2 + \left(\frac{\partial w_h}{\partial y}\right)^2 = \frac{1}{4|K|^2} \left[l_3^2 \left(\frac{\partial w_h}{\partial \lambda_2}\right)^2 + l_2^2 \left(\frac{\partial w_h}{\partial \lambda_3}\right)^2 - 2 l_2 l_3 \cos(\theta_1) \frac{\partial w_h}{\partial \lambda_2} \frac{\partial w_h}{\partial \lambda_3} \right],$$

here $|K|$ is area of triangle K, l_2 and l_3 are opposite edge lenghts of vertices P_2 and P_3 on K, and θ_1 is the angle between l_2 and l_3. Substitute (28) into (29) and integrate on element K

$$\begin{aligned} \iint_K |\nabla w_h|^2 dxdy = & \frac{1}{80|K|} \left[20(1 - \cos(\theta_1)) \left(l_3^2 (Y_1 - Y_2)^2 + l_2^2 (Y_1 - Y_3)^2 \right) \right. \\ & + \left(9((2 - \cos(\theta_1))(l_2^2 + l_3^2) + \cos(\theta_1)(l_2 - l_3)^2 \right) (Y_1 + Y_2 + Y_3)^2 \\ & \left. + 20 \cos(\theta_1) l_2 l_3 (Y_2 - Y_3)^2 \right]. \end{aligned}$$

Since $K \in \mathcal{T}_h$ is regular, then we have

$$\frac{9}{40\sigma^4}(Y_1^2 + Y_2^2 + Y_3^2) \le \iint_K |\nabla w_h|^2 dxdy \le \frac{10\sigma^2}{4}(Y_1^2 + Y_2^2 + Y_3^2).$$

Furthermore, since $\mathcal{T}_h$ is regular, then equivalence between $|\cdot|_{1,V_h}$ with $|\cdot|_1$ is proved.

Now, we prove the equivalence (27). We rewritte (25) as follow

$$|w_h|^2_{1,V_h^*} = \sum_{K\in\mathcal{T}_h} |w_h|^2_{1,V_h^*,K}, \tag{30}$$

where

$$|w_h|^2_{1,V_h^*,K} = \sum_{E\in K\cap\mathcal{E}_{\mathcal{T}^*_{h,v}}} \frac{1}{|E|}\int_E [w_h]^2 ds. \tag{31}$$

Thereby, we only need prove that $|\Pi_v^* w_h|^2_{1,V_h^*,K}$ is equivalent to $|w_h|^2_{1,V_h,K}$. By direct calculation, we have

$$\begin{aligned}|\Pi_v^* w_h|^2_{1,V_h^*,K} &= \frac{1}{3}\left[\tfrac{121}{16}(Y_1+Y_2+Y_3)^2 + (Y_1-Y_2)^2 + (Y_2-Y_3)^2 + (Y_3-Y_1)^2\right]\\ &= \frac{105}{48}(Y_1+Y_2+Y_3)^2 + (Y_1^2+Y_2^2+Y_3^2).\end{aligned}$$

Then we have

$$Y_1^2+Y_2^2+Y_3^2 \le |\Pi_v^* w_h|^2_{1,V_h^*,K} \le \frac{427}{48}(Y_1^2+Y_2^2+Y_3^2). \tag{32}$$

So $|\Pi_v^* w_h|^2_{1,V_h^*}$ is equivalent to $|w_h|^2_{1,V_h}$.

□

Lemma 3.2. *There exist positive constants c_3 and C_3, such that*

$$c_3\|q_h\|_0 \le \|\Pi_p^* q_h\|_0 \le C_3\|q_h\|_0, \quad \forall r_h \in Q_h. \tag{33}$$

Proof. By the definition of $\|\Pi_p^* q_h\|_0$, we have

$$\|\Pi_p^* q_h\|_0^2 = \sum_{K_p^*\in\mathcal{T}^*_{h,p}} |K_p^*| q_h(P)^2 = \sum_{K\in\mathcal{T}_h}\frac{1}{3}|K|\left(q_h^2(P_1)+q_h^2(P_2)+q_h^2(P_3)\right). \tag{34}$$

For further proof, please refer to Reference [27] page 124. □

Now, we prove the continuity for the bilinear form $a_h(\cdot,\cdot)$, $b_h^1(\cdot,\cdot)$ and $b_h^2(\cdot,\cdot)$.

Lemma 3.3. *Assume $\mathcal{T}_h$ is regular, then there exist constants M_1, M_2 and M_3 independent of h, such that for all $\boldsymbol{u} \in \left(H_0^1(\Omega)\cap H_h^2(\Omega)\right)^2$ and $p \in L_0^2(\Omega)\cap H_h^1(\Omega)$,*

$$a_h(\boldsymbol{u},\boldsymbol{v}_h) \le M_1(|\boldsymbol{u}|_1 + h|\boldsymbol{u}|_{2,h})|\boldsymbol{v}_h|_{1,V_h^*} \quad \forall \boldsymbol{v}_h \in (V_h^*)^2, \tag{35}$$

$$b_h^1(\boldsymbol{v}_h,p) \le M_2(\|p\|_0 + h|p|_{1,h})|\boldsymbol{v}_h|_{1,V_h^*} \quad \forall \boldsymbol{v}_h \in (V_h^*)^2, \tag{36}$$

$$b_h^2(\boldsymbol{u},q_h) \le M_3|\boldsymbol{u}|_1\|q_h\|_0 \quad \forall q_h \in Q_h^*, \tag{37}$$

where $|\cdot|_{k,h} = \left(\sum_{K\in\mathcal{T}_h}|\cdot|^2_{k,K}\right)^{1/2}$.

Proof. First, we rewritte

$$a_h(\boldsymbol{u},\boldsymbol{v}_h) = -\sum_{E\in\mathcal{E}_{\mathcal{T}^*_{h,v}}}\int_E \nu\frac{\partial\boldsymbol{u}}{\partial\boldsymbol{n}}\cdot[\boldsymbol{v}_h]\,ds. \tag{38}$$

By Cauchy-Schwartz inequality, we have

$$\left|-\sum_{E\in\mathcal{E}_{\mathcal{T}^*_{h,v}}}\int_E \nu\frac{\partial\boldsymbol{u}}{\partial\boldsymbol{n}}\cdot[\boldsymbol{v}_h]\,ds\right| \le |\boldsymbol{v}_h|_{1,V_h^*}\left(\sum_{E\in\mathcal{E}_{\mathcal{T}^*_{h,v}}}\nu|E|\int_E|\nabla\boldsymbol{u}\cdot\boldsymbol{n}|^2\,ds\right)^{\frac{1}{2}}. \tag{39}$$

According to the trace theorem, we have

$$\int_{E\subset K} w^2 \leq \left(h_K^{-1}|w|_{0,K}^2 + h_K|w|_{1,K}^2\right), \quad w\in H^1(K), \tag{40}$$

where h_K is maximum edge length of triangle K.

By inequality (40), we obtain

$$\sum_{E\in\mathcal{E}_{\mathcal{T}_{h,v}^*}} \nu|E|\int_E |\nabla \boldsymbol{u}\cdot\boldsymbol{n}|^2\,ds \leq M_1\left(|\boldsymbol{u}|_1 + h|\boldsymbol{u}|_{2,h}\right)^2. \tag{41}$$

Thus inequalty (35) follows.

Similarly, $b_h^1(\cdot,\cdot)$ can be rewritten as

$$b_h^1(\boldsymbol{v}_h,p) = \sum_{E\in\mathcal{E}_{\mathcal{T}_{h,v}^*}} \int_E p\,[\boldsymbol{v}_h]\,\boldsymbol{n}ds, \tag{42}$$

furthermore, we have

$$\begin{aligned}\left|\sum_{E\in\mathcal{E}_{\mathcal{T}_{h,v}^*}} \int_E p\,[\boldsymbol{v}_h]\,ds\right| &\leq |\boldsymbol{v}_h|_{1,V_h^*}\left(\sum_{E\in\mathcal{E}_{\mathcal{T}_{h,v}^*}} |E|\int_E |p|^2 ds\right)^{\frac{1}{2}}\\ &\leq M_2(\|p\|_0 + h|p|_{1,h})|\boldsymbol{v}_h|_{1,V_h^*}.\end{aligned}$$

Finally, for bilinear $b^2(\cdot,\cdot)$, by using Cauchy-Schwartz inequality

$$b_h^2(\boldsymbol{u},q_h) \leq \left|\sum_{K_q^*\in\mathcal{T}_{h,p}^*}\int_{K_q^*} \operatorname{div}(\boldsymbol{u})q_h dx\right| \leq ||\operatorname{div}(\boldsymbol{u})||_0\|q_h\|_0 \leq M_3|\boldsymbol{u}|_1\|q_h\|_0.$$

□

First, we introduce the operator Π_h from V_h to V_h

$$\Pi_h u_h = u_h^l + \tfrac{55}{36}u_h^b. \tag{43}$$

Then, we have the follow equivalence.

Lemma 3.4. *For any $\boldsymbol{v}_h\in(V_h)^2$, we have*

$$b_h^1(\Pi_v^*\boldsymbol{v}_h,q_h) = -b(\Pi_h\boldsymbol{v}_h,q_h), \quad \forall q_h\in Q_h. \tag{44}$$

Proof. Firstly, we prove that the operator Π_v^* and Π_h satisfies the following orthogonality,

$$\iint_K \left(\Pi_h v_h - \Pi_v^* v_h\right)dxdy = 0, \quad \forall v_h\in\mathbb{P}_{1+b},\ K\in\mathcal{T}_h. \tag{45}$$

By the area coordinate integration formula, we have

$$\begin{aligned}\iint_K \Pi_h v_h dxdy =& \frac{1}{3}|K|\sum_{i=1}^3 v_h^l|_K(P_i) + 2|K|\frac{55}{36}\times 27\times\frac{1}{5!}v_h^b|_K(O)\\ =&\frac{|K|}{3}\sum_{i=1}^3 v_h^l|_K(P_i) + \frac{11|K|}{16}v_h^b|_K(O).\end{aligned} \tag{46}$$

In addition, due to $\Pi_v^* v_h$ is piecewise constant function, we have

(47)
$$\iint_K \Pi_v^* v_h dxdy = \frac{1}{4}|K| \sum_{i=1}^{3} v_h^l|_K(P_i) + \frac{1}{4}|K| \left(\frac{1}{3} \sum_{i=1}^{3} v_h^l|_K(P_i) + \frac{11}{4} v_h^b|_K(O) \right)$$
$$= \frac{1}{3}|K| \sum_{i=1}^{3} v_h^l|_K(P_i) + \frac{11}{16}|K| v_h^b|_K(O).$$

Apply Green's formula to (6) and (17),

$$b(\Pi_h \boldsymbol{v}_h, q_h) = \iint_\Omega q_h \operatorname{div}(\Pi_h \boldsymbol{v}_h) dxdy = -\sum_{K \in \mathcal{T}_h} \iint_K \nabla q_h \cdot \Pi_h \boldsymbol{v}_h dxdy, \tag{48}$$

and

$$b_h^1(\Pi_v^* \boldsymbol{v}_h, q_h) = \sum_{K_v^* \in \mathcal{T}_{h,v}^*} \Pi_v^* \boldsymbol{v}_h \cdot \int_{\partial K_v^*} q_h \boldsymbol{n} ds = \sum_{K_v^* \in \mathcal{T}_{h,v}^*} \Pi_v^* \boldsymbol{v}_h \cdot \iint_{K_v^*} \nabla q_h dxdy. \tag{49}$$

Due to (45)

$$\begin{aligned} b(\Pi_h \boldsymbol{v}_h, q_h) + b_h^1(\Pi_v^* \boldsymbol{v}_h, q_h) &= \sum_{K_v^* \in \mathcal{T}_{h,v}^*} \Pi_v^* \boldsymbol{v}_h \cdot \iint_{K_v^*} \nabla q_h dxdy \\ &\quad - \sum_{K \in \mathcal{T}_h} \iint_K \nabla q_h \cdot \Pi_h \boldsymbol{v}_h dxdy \\ &= \sum_{K \in \mathcal{T}_h} \nabla q_h \cdot \iint_K \left(\Pi_v^* \boldsymbol{v}_h - \Pi_h \boldsymbol{v}_h \right) dxdy = 0. \end{aligned}$$

□

Corollary 3.1. *There exists a positive γ_1 independent of h, such that*

$$\sup_{\boldsymbol{v}_h \in (V_h^*)^2 \setminus \{\boldsymbol{0}\}} \frac{b_h^1(\boldsymbol{v}_h, q_h)}{|\boldsymbol{v}_h|_{1,V_h^*}} \geq \gamma_1 \|q_h\|_0, \quad \forall q_h \in Q_h. \tag{50}$$

Proof. Considering Π_h is a linear one-to-one mapping of V_h onto itself, there exist constants c_4 and C_4, such that

$$c_4 |\boldsymbol{u}_h|_1 \leq |\Pi_h \boldsymbol{u}_h|_1 \leq C_4 |\boldsymbol{u}_h|_1. \tag{51}$$

By Lemma 3.4, and combining equivalence between (26) with (27), we obtain

$$\begin{aligned} \sup_{\boldsymbol{v}_h \in (V_h^*)^2 \setminus \{\boldsymbol{0}\}} \frac{b_h^1(\boldsymbol{v}_h, q_h)}{|\boldsymbol{v}_h|_{1,V_h^*}} &\geq \sup_{\widetilde{\boldsymbol{v}}_h \in (V_h)^2 \setminus \{\boldsymbol{0}\}} \frac{b_h^1(\Pi_v^* \widetilde{\boldsymbol{v}}_h, q_h)}{|\Pi_v^* \widetilde{\boldsymbol{v}}_h|_{1,V_h^*}} \\ &\geq \frac{1}{C_1 C_2 C_4} \sup_{\widetilde{\boldsymbol{v}}_h \in (V_h)^2 \setminus \{\boldsymbol{0}\}} \frac{b(\Pi_h \widetilde{\boldsymbol{v}}_h, q_h)}{|\Pi_h \widetilde{\boldsymbol{v}}_h|_1} \geq \frac{\gamma_0}{C_1 C_2 C_4} \|q_h\|_0. \end{aligned}$$

□

Lemma 3.5. *For any $\boldsymbol{v}_h \in (V_h)^2$, we have*

$$b(\Pi_h \boldsymbol{v}_h, q_h) = b_h^2(\boldsymbol{v}_h, \Pi_p^* q_h), \quad \forall q_h \in Q_h. \tag{52}$$

Proof. Considering $\Pi_h \boldsymbol{u}_h = \boldsymbol{u}_h^l + \frac{55}{36}\boldsymbol{u}_h^b$,

$$
\begin{aligned}
b(\Pi_h \boldsymbol{u}_h, q_h) &= \iint_\Omega q_h \operatorname{div}(\boldsymbol{u}_h) dxdy \\
&= \sum_{K\in\mathcal{T}_h} \left(\iint_K q_h \operatorname{div}(\boldsymbol{u}_h^l) dxdy + \tfrac{55}{36} \iint_K q_h \operatorname{div}(\boldsymbol{u}_h^b) dxdy \right).
\end{aligned} \tag{53}
$$

Similarly, we have

$$
\begin{aligned}
b_h^2(\boldsymbol{u}_h, \Pi_p^* q_h) &= \sum_{K_q^*\in\mathcal{T}_{h,p}^*} \iint_{K_q^*} \operatorname{div}(\boldsymbol{u}_h)\Pi_p^* q_h dxdy \\
&= \sum_{K\in\mathcal{T}_h} \left(\iint_K \operatorname{div}(\boldsymbol{u}_h^l)\Pi_p^* q_h dxdy + \iint_K \operatorname{div}(\boldsymbol{u}_h^b)\Pi_p^* q_h dxdy \right).
\end{aligned}
$$

For the linear part, considering $\operatorname{div}(\boldsymbol{u}_h^l)$ is constant on K, then

$$
\iint_K \operatorname{div}(\boldsymbol{u}_h^l) q_h dxdy - \iint_K \operatorname{div}(\boldsymbol{u}_h^l)\Pi_p^* q_h dxdy = \operatorname{div}(\boldsymbol{u}_h^l) \iint_K \left(q_h - \Pi_p^* q_h\right) dxdy = 0.
$$

For the bubble part, by simple calculation, we have

$$
\tfrac{55}{36} \iint_K q_h \operatorname{div}(\Pi_h \boldsymbol{u}_h^b) dxdy = \frac{11|K|}{16}\boldsymbol{u}_h^b \cdot \nabla q_h = \iint_K \operatorname{div}(\boldsymbol{u}_h^b)\Pi_p^* q_h dxdy. \tag{54}
$$

Then equation (52) holds. □

Corollary 3.2. *There exists a positive γ_2 independent of h, such that*

$$
\sup_{\boldsymbol{v}_h\in(V_h)^2\backslash\{\boldsymbol{0}\}} \frac{b_h^2(\boldsymbol{v}_h, q_h)}{|\boldsymbol{v}_h|_1} \geq \gamma_2 \|q_h\|_0, \quad \forall q_h \in Q_h^*. \tag{55}
$$

Proof. By Lemma 3.5, Lemma 3.2 and (51), for any $q_h \in Q_h$, we have

$$
\begin{aligned}
\sup_{\boldsymbol{v}_h\in(V_h)^2\backslash\{\boldsymbol{0}\}} \frac{b_h^2(\boldsymbol{v}_h, \Pi_p^* q_h)}{|\boldsymbol{v}_h|_1} &\geq \sup_{\boldsymbol{v}_h\in(V_h)^2\backslash\{\boldsymbol{0}\}} \frac{b_h^2(\Pi_h \boldsymbol{v}_h, q_h)}{|\boldsymbol{v}_h|_1} \\
&\geq \frac{1}{c_4} \sup_{\boldsymbol{v}_h\in(V_h)^2\backslash\{\boldsymbol{0}\}} \frac{b(\Pi_h \boldsymbol{v}_h, q_h)}{|\Pi_h \boldsymbol{v}_h|_1} \geq \frac{\gamma_0}{c_4}\|q_h\|_0 \geq \frac{c_3\gamma_0}{c_4}\|\Pi_p^* q_h\|_0.
\end{aligned}
$$

Then the Inf-Sup condition of $b_h^2(\boldsymbol{v}_h, q_h)$ is proved.

□

Remark 3.1. *According to Lemma 3.4 and Lemma 3.5, we have,*

$$
b_h^1(\Pi_v^* \boldsymbol{v}_h, q_h) = b(\Pi_h \boldsymbol{v}_h, q_h) = b_h^2(\boldsymbol{v}_h, \Pi_p^* q_h). \tag{56}
$$

When the scheme (20) is expressed as the block 2×2 linear systems

$$
\begin{bmatrix} A & B_1^T \\ B_2 & O \end{bmatrix} \begin{bmatrix} x \\ y \end{bmatrix} = \begin{bmatrix} F \\ 0 \end{bmatrix},
$$

where A, B_1 and B_2 denote the matrix corresponding to the bilinear form $a_h(\cdot,\cdot)$, $b_h^1(\cdot,\cdot)$ and $b_h^2(\cdot,\cdot)$, and O is the null matrix, we can find $B_1 \neq B_2$. However (56) shows that although $B_1 \neq B_2$, there exists a simple linear transformation G such that $GB_1^T = B_2^T$.

Now, we prove that $a_h(\cdot, \Pi_v^* \cdot)$ satisfies the following positive definiteness.

Theorem 3.1. *If $\mathcal{T}_h$ is regular, and $\theta_{min,K} > 11.62°$ for all $K \in \mathcal{T}_h$, then there exist positive c such that*

$$a_h(\boldsymbol{u}_h, \Pi_v^* \boldsymbol{u}_h) \geq c|\boldsymbol{u}_h|_1^2, \tag{57}$$

where $\theta_{min,K}$ is the smallest angle of K.

Proof. With the help of operator Π_v^*, we can rewritte the bilinear form (16) as follow

$$a_h(\boldsymbol{u}_h, \Pi_v^* \boldsymbol{u}_h) = \sum_{K \in \mathcal{T}_h} a_h^K(\boldsymbol{u}_h, \Pi_v^* \boldsymbol{u}_h),$$

where

$$\begin{aligned}
&a_h^K(\boldsymbol{u}_h, \Pi_v^* \boldsymbol{u}_h)\\
=&-\sum_{E \in \mathcal{E}_{\mathcal{T}_{h,v}^*}} \int_{E \subset K} \nu \frac{\partial \boldsymbol{u}_h}{\partial \boldsymbol{n}} [\Pi_v^* \boldsymbol{u}_h] \, ds\\
=&-\sum_{E \in \mathcal{E}_{\mathcal{T}_{h,v}^*}} \int_{E \subset K} \nu \frac{\partial u_h^x}{\partial \boldsymbol{n}} [\Pi_v^* u_h^x] \, ds - \sum_{E \in \mathcal{E}_{\mathcal{T}_{h,v}^*}} \int_{E \subset K} \nu \frac{\partial u_h^y}{\partial \boldsymbol{n}} [\Pi_v^* u_h^y] \, ds\\
=&\nu I_K(u_h^x, \Pi_v^* u_h^x) + \nu I_K(u_h^y, \Pi_v^* u_h^y).
\end{aligned}$$

Obviously, in order to obtain the coercivity of $a_h^K(\boldsymbol{u}_h, \Pi_v^* \boldsymbol{u}_h)$, one only need to prove

$$I_K(v_h, \Pi_v^* v_h) \geq c|v_h|_1^2, \quad \forall v_h \in V_h. \tag{58}$$

By computation, we have

$$I_K(v_h, \Pi_v^* v_h) = -\sum_{E \in \mathcal{E}_{\mathcal{T}_{h,v}^*}} \int_{E \subset K} \frac{\partial v_h}{\partial \boldsymbol{n}} [\Pi_v^* v_h] \, ds = \boldsymbol{Y}^T D A \boldsymbol{Y}, \tag{59}$$

where $\boldsymbol{Y} = [Y_1, Y_2, Y_3]^T$,

$$D = \frac{1}{12}\begin{pmatrix} 19, & 7, & 7 \\ 7, & 19, & 7 \\ 7, & 7, & 19 \end{pmatrix}, \quad A = \frac{1}{8}\begin{pmatrix} 7(\alpha_2+\alpha_3), & 3\alpha_2-\alpha_3, & 3\alpha_3-\alpha_2 \\ 3\alpha_1-\alpha_3, & 7(\alpha_1+\alpha_3), & 3\alpha_3-\alpha_1 \\ 3\alpha_1-\alpha_2, & 3\alpha_2-\alpha_1, & 7(\alpha_1+\alpha_2) \end{pmatrix},$$

here $\alpha_i = \cot(\theta_i), i = 1, 2, 3$. Considering

$$I_K(v_h, \Pi_{v,\frac{11}{4}}^* v_h) = \frac{1}{2}\left(\boldsymbol{Y}^T D A \boldsymbol{Y} + \boldsymbol{Y}^T A^T D^T \boldsymbol{Y}\right) = \boldsymbol{Y}^T B \boldsymbol{Y}, \tag{60}$$

where B is the symmetrized quadratic form. It is easy to verify that when K is a regular triangle, the matrix B is positive definite, that is when $\alpha_1 = \alpha_2 = \alpha_3 = \sqrt{1/3}$, $\det(B) = \frac{99}{64}\sqrt{3}$, and the smallest eigenvalue of B is 0.866. By computation, we have

$$\det(B) = \frac{9}{512}\left(-4\left(\alpha_1+\alpha_2+\alpha_3\right)^3 - 27\alpha_1\alpha_2\alpha_3 + 103\left(\alpha_1+\alpha_2+\alpha_3\right)\right). \tag{61}$$

Without loss of generality, let $\theta_1 \leq \theta_2 \leq \theta_3$, and $0 < \alpha_2 < \alpha_1$. Since $\alpha_3 = (1-\alpha_1\alpha_2)/(\alpha_1+\alpha_2)$, we have

$$\begin{aligned}
\det(B) =& \frac{9}{512}(\alpha_1+\alpha_2)^{-3}((194\alpha_1\alpha_2 + 258\alpha_1\alpha_2^3 + 258\alpha_1^3\alpha_2 - 12\alpha_1\alpha_2^5 - 12\alpha_1^5\alpha_2\\
&+ 91\alpha_1^2 + 91\alpha_2^2 + 91\alpha_1^4 + 91\alpha_2^4 - 4\alpha_1^6 - 4\alpha_2^6 + 3\alpha_1^2\alpha_2^4 + 26\alpha_1^3\alpha_2^3\\
&+ 3\alpha_1^4\alpha_2^2 + 322\alpha_1^2\alpha_2^2 - 4)),
\end{aligned}$$

when fixed α_1, then $\sqrt{\alpha_1^2+1}-\alpha_1 \le \alpha_2 \le \alpha_1$

$$\begin{aligned}\frac{\partial \det(B)}{\partial \alpha_2} =& \frac{9}{512(\alpha_1+\alpha_2)^4}(\alpha_2^2+2\alpha_1\alpha_2-1)(15\alpha_1^3(\alpha_1+2\alpha_2)-12\alpha_2^3(2\alpha_1+\alpha_2)\\ &+(79)(\alpha_1+\alpha_2)^2-9\alpha_1^2\alpha_2^2+24\alpha_1\alpha_2-12)\\ =& \frac{9}{512(\alpha_1+\alpha_2)^4}(\alpha_2^2+2\alpha_1\alpha_2-1)((79+15\alpha_1^2-24\alpha_2^2)(\alpha_1+\alpha_2)^2\\ &+12(1+\alpha_2^2)(\alpha_2^2+2\alpha_1\alpha_2-1)),\end{aligned}$$

when $\alpha_2=\sqrt{\alpha_1^2+1}-\alpha_1$, $\det(B)$ reach the smallest value. So,

$$\min(\det(B)) = \frac{9}{1024\alpha_2^3}\left(255\alpha_2^4+96\alpha_2^2-1\right). \tag{62}$$

By simple continuity argument, when

$$\theta_{min} \ge 180^\circ - 2\,\mathrm{arccot}\left(\sqrt{\tfrac{4\sqrt{165}-47}{255}}\right) \approx 11.62^\circ, \tag{63}$$

the smallest eigenvalue of B is positive. So when $\theta_{min,K} > 11.62^\circ$, by equivalence of discrete norm, we have

$$I_K(v_h, \Pi_v^* v_h) = \boldsymbol{Y}^T B \boldsymbol{Y} \ge \lambda_{min}^B (Y_1^2+Y_2^2+Y_3^2) \ge c|v_h|_{1,K}^2, \tag{64}$$

where λ_{min}^B is the smallest eigenvalue of B. Further

$$a_h(\boldsymbol{u}_h, \Pi_v^*\boldsymbol{u}_h) = \sum_{K\in\mathcal{T}_h} I_K(u_h^x, \Pi_v^* u_h^x) + \sum_{K\in\mathcal{T}_h} I_K(u_h^y, \Pi_v^* u_h^y) \ge c|\boldsymbol{u}_h|_1^2.$$

Then we finish the proof. □

Finally, we give the existence and uniqueness of the solution of MINI mixed finite volume methods.

Theorem 3.2. *Assume that $\mathcal{T}_h$ is quasi-uniform, $\theta_{min,K} > 11.62^\circ$ for all $K\in\mathcal{T}_h$. Then for $f \in L^2(\Omega)$ the MINI mixed FVEMs (23) has a unique solution.*

Proof. Considering,

$$b_h^1(\Pi_v^*\boldsymbol{v}_h, q_h) = -b_h^2(\boldsymbol{v}_h, \Pi_p^* q_h). \tag{65}$$

Furthermore, we have when $\theta_{min,K} > 11.62^\circ$, $a_h(\boldsymbol{u}_h, \Pi_v^*\boldsymbol{u}_h) \ge c|\boldsymbol{u}_h|_1^2$, and $b_h^2(\boldsymbol{u}_h, \Pi_p^* p_h)$ satifies Inf-Sup condition. By the theory of saddle-point problem[19, 6], we know that the solution of (23) exists uniquely. □

4. Convergence analysis

Before the error analysis, we introduce the null space corresponding to the continuum problem, the finite element methods, and the finite volume methods respectively as follows

$$Z := \left\{\boldsymbol{u} \in (H_0^1(\Omega))^2 : b(\boldsymbol{u}, p) = 0,\ \forall p \in L_0^2(\Omega)\right\}, \tag{66}$$

$$Z_h := \left\{\boldsymbol{u}_h \in (V_h)^2 : b(\boldsymbol{u}_h, p_h) = 0,\ \forall p_h \in Q_h\right\}, \tag{67}$$

$$Z_h^2 := \left\{\boldsymbol{u}_h \in (V_h)^2 : b_h^2(\boldsymbol{u}_h, p_h) = 0,\ \forall p_h \in Q_h^*\right\}. \tag{68}$$

In the paper [1], D. N. Arnold et al. construct the operator $\Pi_{\mathbb{P}_{1+b}} : (H_0^1)^2 \to (V_h)^2$ that satisfies for any $\boldsymbol{v} \in (H_0^1)^2$

$$\int_\Omega \operatorname{div}(\boldsymbol{v} - \Pi_{\mathbb{P}_{1+b}}\boldsymbol{v})q_h = 0, \quad \forall q_h \in Q_h, \tag{69}$$

$$|\Pi_{\mathbb{P}_{1+b}}\boldsymbol{v}|_1 \le c|\boldsymbol{v}|_1. \tag{70}$$

Relation (69) imply that $\Pi_{\mathbb{P}_{1+b}}$ can project any element of Z into Z_h. And operator $\Pi_{\mathbb{P}_{1+b}}$ has the following interpolation estimate [19]

$$\left|\boldsymbol{v} - \Pi_{\mathbb{P}_{1+b}}\boldsymbol{v}\right|_m \le Ch^{2-m}|\boldsymbol{v}|_2, \quad \forall \boldsymbol{v} \in (H^2(\Omega))^2, \quad m = 0, 1. \tag{71}$$

Now we introduce interpolation operator $\widehat{\Pi}_{\mathbb{P}_{1+b}} : (H_0^1(\Omega))^2 \to (V_h)^2$, which is defined as $\widehat{\Pi}_{\mathbb{P}_{1+b}} = \Pi_h^{-1} \circ \Pi_{\mathbb{P}_{1+b}}$. By simple computation, we can prove that $\widehat{\Pi}_{\mathbb{P}_{1+b}}$ can project any element of Z into Z_h^2. Since operator $\widehat{\Pi}_{\mathbb{P}_{1+b}}$ only adjusts the bubble term coefficient of operator $\Pi_{\mathbb{P}_{1+b}}$, based on similar arguments, we can get the following interpolation error estimates.

Lemma 4.1. *Let $\mathcal{T}_h$ be regular partition. For any $\boldsymbol{u} \in (H^2 \cap H_0^1)^2$, the interpolation operator $\widehat{\Pi}_{\mathbb{P}_{1+b}}$ satisfies*

$$\left|\boldsymbol{v} - \widehat{\Pi}_{\mathbb{P}_{1+b}}\boldsymbol{v}\right|_m \le Ch^{2-m}|\boldsymbol{v}|_2, \quad m = 0, 1. \tag{72}$$

Now, we proof the error estimation.

Theorem 4.1. *Let $(\boldsymbol{u}, p) \in \left((H_0^1 \cap H^2)^2, L_0^2 \cap H^1\right)$ be the solution of problem (1), and $(\boldsymbol{u}_h, p_h) \in (V_h)^2 \times Q_h$ is the solution of (20). If the partition $\mathcal{T}_h$ is regular, and $\theta_{min,K} > 11.62^\circ$, there exists a constant C such that*

$$|\boldsymbol{u} - \boldsymbol{u}_h|_1 + \|p - p_h\|_0 \le Ch\left(\|\boldsymbol{u}\|_2 + \|p\|_1\right). \tag{73}$$

Proof. By (1) and (20), we have

$$a_h(\boldsymbol{u} - \boldsymbol{u}_h, \boldsymbol{v}_h) + b_h^1(\boldsymbol{v}_h, p - p_h) = 0, \quad \forall \boldsymbol{v}_h \in (V_h^*)^2, \tag{74}$$

$$b_h^2(\boldsymbol{u} - \boldsymbol{u}_h, q_h) = 0, \quad \forall q_h \in Q_h^*. \tag{75}$$

Let $\boldsymbol{\xi} = \boldsymbol{u} - \widehat{\Pi}_{\mathbb{P}_{1+b}}\boldsymbol{u}$, $\boldsymbol{\xi}_h = \boldsymbol{u}_h - \widehat{\Pi}_{\mathbb{P}_{1+b}}\boldsymbol{u}$, $\eta = p - \Pi_{\mathbb{P}_1}p$ and $\eta_h = p_h - \Pi_{\mathbb{P}_1}p$

$$\begin{aligned} a_h(\boldsymbol{\xi}_h, \boldsymbol{v}_h) + b_h^1(\boldsymbol{v}_h, \eta_h) &= a_h(\boldsymbol{\xi}, \boldsymbol{v}_h) + b_h^1(\boldsymbol{v}_h, \eta), \quad && \forall \boldsymbol{v}_h \in (V_h^*)^2, \\ b_h^2(\boldsymbol{\xi}, q_h) &= b_h^2(\boldsymbol{\xi}_h, q_h) = 0, && \forall q_h \in Q_h^*. \end{aligned}$$

Taking $\boldsymbol{v}_h = \Pi_v^*\boldsymbol{\xi}_h$ and $q_h = \Pi_p^*\eta_h$

$$b_h^1(\Pi_v^*\boldsymbol{\xi}_h, \eta_h) = b_h^2(\boldsymbol{\xi}_h, \Pi_p^*\eta_h), \tag{76}$$

then

$$a_h(\boldsymbol{\xi}_h, \Pi_v^*\boldsymbol{\xi}_h) = a_h(\xi, \Pi_v^*\boldsymbol{\xi}_h) + b_h^1(\Pi_v^*\boldsymbol{\xi}_h, \eta),$$

First, we give the error estimate for the velocity.

By interpolation estimations of operator $\widehat{\Pi}_{\mathbb{P}_{1+b}}$ and operator $\Pi_{\mathbb{P}_1}$

$$a_h(\xi, \Pi_v^*\boldsymbol{\xi}_h) \le C|\xi|_1|\boldsymbol{\xi}_h|_1 \le Ch|\boldsymbol{u}|_2|\boldsymbol{\xi}_h|_1, \tag{77}$$

$$b_h^1(\Pi_v^*\boldsymbol{\xi}_h, \eta) \le C|\eta|_0|\boldsymbol{\xi}_h|_1 \le Ch|p|_1|\boldsymbol{\xi}_h|_1. \tag{78}$$

Considering the coercivity of bilinear form $a_h(\cdot, \Pi_v^*\cdot)$, we obtain

$$|\boldsymbol{\xi}_h|_1^2 \le a_h(\boldsymbol{\xi}_h, \Pi_v^*\boldsymbol{\xi}_h) = a_h(\xi, \Pi_v^*\boldsymbol{\xi}_h) + b_h^1(\Pi_v^*\boldsymbol{\xi}_h, \eta) \le Ch\left(|\boldsymbol{u}|_2 + |p|_1\right)|\boldsymbol{\xi}_h|_1,$$

then

$$|\boldsymbol{u}-\boldsymbol{u}_h|_1 \le |\boldsymbol{u}-\widehat{\Pi}_{\mathbb{P}_{1+b}}\boldsymbol{u}|_1 + |\widehat{\Pi}_{\mathbb{P}_{1+b}}\boldsymbol{u}-\boldsymbol{u}_h|_1 \le Ch\left(|\boldsymbol{u}|_2+|p|_1\right). \tag{79}$$

Now, we give the error estimate for the pressure. By (74), we have

$$b_h^1(\boldsymbol{v}_h,\eta_h) = a_h(\boldsymbol{u}-\boldsymbol{u}_h,\boldsymbol{v}_h) + b_h^1(\boldsymbol{v}_h,\eta). \tag{80}$$

According to the continuity of bilinear form $a_h(\cdot,\cdot)$ and $b_h^1(\cdot,\cdot)$

$$a_h(\boldsymbol{u}-\boldsymbol{u}_h,\boldsymbol{v}_h) \le M_1|\boldsymbol{u}-\boldsymbol{u}_h|_1|\boldsymbol{v}_h|_1, \tag{81}$$

$$b_h^1(\boldsymbol{v}_h,\eta) \le M_2|\eta|_0|\boldsymbol{v}_h|_1 \le M_2h|p|_1|\boldsymbol{v}_h|_1. \tag{82}$$

Combined with the Inf-Sup condition of bilinear form $b_h^1(\cdot,\cdot)$

$$\|\eta_h\| \le \frac{1}{\gamma_1}\sup_{\boldsymbol{v}_h\in(V_h^*)^2}\frac{b_h^1(\boldsymbol{v}_h,\eta_h)}{|\boldsymbol{v}_h|_{1,V_h^*}} \le C|\boldsymbol{u}-\boldsymbol{u}_h|_1 + Ch|p|_1 \le Ch\left(|\boldsymbol{u}|_2+|p|_1\right).$$

By the triangle inequality

$$\|p-p_h\|_0 \le \|p-\Pi_{\mathbb{P}_1}p\|_0 + \|\Pi_{\mathbb{P}_1}p-p_h\|_0 \le Ch\left(|\boldsymbol{u}|_2+|p|_1\right). \tag{83}$$

Combining (79) and (83), we have

$$|\boldsymbol{u}-\boldsymbol{u}_h|_1 + \|p-p_h\|_0 \le Ch\left(\|\boldsymbol{u}\|_2+\|p\|_1\right). \tag{84}$$

□

5. Numerical experiments

In this section, three benchmark test, which come from reference [14], are taken to illustrate the theoretical results. In all test problems, the Stokes equation (1) is considered in unit square domain $\Omega=(0,1)^2$, and the exact solution of pressure have vanishing mean over the domain. We use uniform right triangular meshes in the following test. The discrete errors for H^1-semi-norm and L^2-norm are calculated as follows

$$|\boldsymbol{u}-\boldsymbol{u}_h|_1 := \left(\sum_{K\in\mathcal{T}_h}\iint_K\left[\left(\frac{\partial\boldsymbol{u}}{\partial x}-\frac{\partial\boldsymbol{u}_h}{\partial x}\right)^2+\left(\frac{\partial\boldsymbol{u}}{\partial y}-\frac{\partial\boldsymbol{u}_h}{\partial y}\right)^2\right]dxdy\right)^{\frac{1}{2}},$$

$$\|\boldsymbol{u}-\boldsymbol{u}_h\|_0 := \left(\sum_{K\in\mathcal{T}_h}\iint_K(\boldsymbol{u}-\boldsymbol{u}_h)^2\,dxdy\right)^{\frac{1}{2}},$$

$$\|p-p_h\|_0 := \left(\sum_{K\in\mathcal{T}_h}\iint_K(p-p_h)^2\,dxdy\right)^{\frac{1}{2}}.$$

The rate of convergence is given by the following formula:

$$\text{Rate } = \log\left(\frac{E(h_1)}{E(h_2)}\right)\log\left(\frac{h_2}{h_1}\right)^{-1},$$

where h_1,h_2 denote the mesh sizes of the successive meshes, and $E(h_1)$, $E(h_2)$ are the corresponding error.

Example 1 Enclosed vortex with non-polynomial solution

In this example, we test the schemes by enclosed vortex problem with non-polynomial solutions. Consider right-hand side of equation (1) as

$$f^x = -4\pi^2\nu\sin(2\pi y)[2\cos(2\pi x)-1] + 4\pi^2\sin(2\pi x),$$
$$f^y = 4\pi^2\nu\sin(2\pi x)[2\cos(2\pi y)-1] - 4\pi^2\sin(2\pi y),$$

and the corresponding exact solution are

$$u^x(x,y) = \sin(2\pi y)[1-\cos(2\pi x)],$$
$$u^y(x,y) = \sin(2\pi x)[\cos(2\pi y)-1],$$
$$p(x,y) = 2\pi[\cos(2\pi y)-\cos(2\pi x)].$$

TABLE 1. Errors and convergence rates for Example 1.

h	$\\|\boldsymbol{u}-\boldsymbol{u}_h\\|_{0,h}$	Rate	$\|\boldsymbol{u}-\boldsymbol{u}_h\|_{1,h}$	Rate	$\\|p-p_h\\|_{0,h}$	Rate
1/6	1.6909×10^{-1}	–	3.4796×10^{-0}	–	1.5143×10^{-0}	–
1/12	4.3483×10^{-2}	1.9593	1.7845×10^{-0}	0.9635	4.5513×10^{-1}	1.7343
1/24	1.0845×10^{-2}	2.0035	8.9566×10^{-1}	0.9945	1.4570×10^{-1}	1.6433
1/48	2.7009×10^{-3}	2.0054	4.4786×10^{-1}	0.9999	4.9335×10^{-2}	1.5623
1/96	6.7356×10^{-4}	2.0036	2.2383×10^{-1}	1.0006	1.7113×10^{-2}	1.5275
1/192	1.6815×10^{-4}	2.0020	1.1188×10^{-1}	1.0005	5.9945×10^{-3}	1.5134

Example 2 Lid-driven cavity flow with polynomial solution

In this example, we test the schemes by lid-driven cavity flow problem with polynomial solutions. Consider right-hand side of equation (1) as

$$f^x = 0,$$
$$f^y = \nu\left[(12x-6)\left(y^4-y^2\right)+\left(8x^3-12x^2+4x\right)\left(6y^2-1\right)+0.4\left(6x^5-15x^4+10x^3\right)\right],$$

and the corresponding exact solution is

$$u^x(x,y) = \left(x^4-2x^3+x^2\right)\left(2y^3-y\right),$$
$$u^y(x,y) = -\left(2x^3-3x^2+x\right)\left(y^4-y^2\right),$$
$$p(x,y) = \nu\left[\left(4x^3-6x^2+2x\right)\left(2y^3-y\right)+0.4\left(6x^5-15x^4+10x^3\right)y-0.1\right].$$

TABLE 2. Errors and convergence rates for Example 2.

h	$\\|\boldsymbol{u}-\boldsymbol{u}_h\\|_{0,h}$	Rate	$\|\boldsymbol{u}-\boldsymbol{u}_h\|_{1,h}$	Rate	$\\|p-p_h\\|_{0,h}$	Rate
1/6	1.6366×10^{-3}	–	5.4723×10^{-2}	–	7.4636×10^{-2}	–
1/12	4.1454×10^{-4}	1.9811	2.6491×10^{-2}	1.0467	2.4116×10^{-2}	1.6299
1/24	1.0177×10^{-4}	2.0262	1.2893×10^{-2}	1.0389	7.1561×10^{-3}	1.7528
1/48	2.5074×10^{-5}	2.0211	6.3645×10^{-3}	1.0185	4.9335×10^{-3}	1.7581
1/96	6.2179×10^{-6}	2.0117	3.1647×10^{-3}	1.0080	6.4426×10^{-4}	1.7154
1/192	1.5480×10^{-6}	2.0060	1.5786×10^{-3}	1.0035	2.0448×10^{-4}	1.6557

Example 3 Corner flow with polynomial solution

In this example, we test the schemes by corner flow problem with polynomial solutions. Consider right-hand side of equation (1) as

$$f^x = -\nu\left[\sin(xy)x\left(x^2+y^2\right)-2\cos(xy)y\right]-\sin(xy)y,$$
$$f^y = \nu\left[\sin(xy)y\left(x^2+y^2\right)-2\cos(xy)x\right]-\sin(xy)x,$$

and the corresponding exact solution is

$$u^x(x,y) = \left(x^4-2x^3+x^2\right)\left(2y^3-y\right),$$
$$u^y(x,y) = -\left(2x^3-3x^2+x\right)\left(y^4-y^2\right),$$
$$p(x,y) = \nu\left[\left(4x^3-6x^2+2x\right)\left(2y^3-y\right)+0.4\left(6x^5-15x^4+10x^3\right)y-0.1\right].$$

TABLE 3. Errors and convergence rates for Example 3.

h	$\|\boldsymbol{u}-\boldsymbol{u}_h\|_{0,h}$	Rate	$\|\boldsymbol{u}-\boldsymbol{u}_h\|_{1,h}$	Rate	$\|p-p_h\|_{0,h}$	Rate
1/6	2.9182×10^{-3}	–	1.2966×10^{-1}	–	5.2445×10^{-2}	–
1/12	7.0837×10^{-4}	2.0425	6.4367×10^{-2}	1.0103	1.7623×10^{-2}	1.5734
1/24	1.7449×10^{-4}	2.0214	3.2029×10^{-2}	1.0070	6.2350×10^{-3}	1.4990
1/48	4.3360×10^{-5}	2.0087	1.5971×10^{-2}	1.0039	2.2042×10^{-3}	1.5001
1/96	1.0812×10^{-5}	2.0037	7.9740×10^{-3}	1.0021	7.7816×10^{-4}	1.5021
1/192	2.6997×10^{-6}	2.0018	3.9841×10^{-3}	1.0010	2.7472×10^{-4}	1.5021

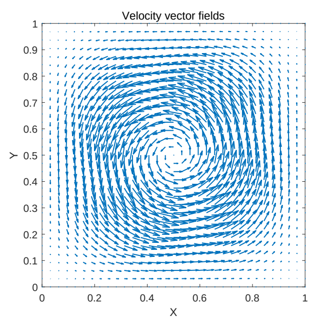

(a) Test Problems 1

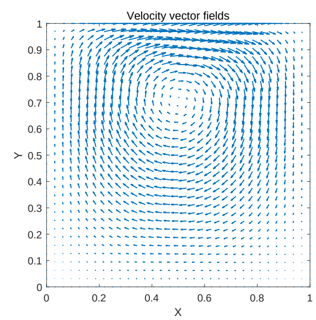

(b) Test Problems 2

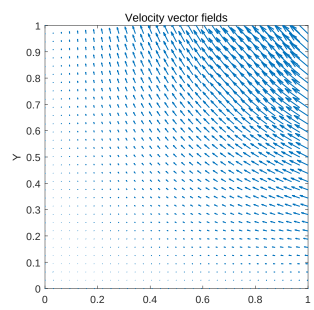

(c) Test Problems 3

FIGURE 3. Velocity vector fields for the benchmark test problems.

The results of the three benchmark tests are shown in Table 1, Table 2 and Table 3, respectively. At the same time, the velocity vector fields corresponding the three problems on the $2\times32\times32$ meshes are showen in Figure 3. As shown by data, the convergence order of velocity in L^2-norm is $O(h^2)$ in H^1-norm is $O(h)$ and convergence order of pressure in L^2-norm is about $O(h^{3/2})$. The convergence of MINI-FVEM are consistent with MINI mixed finite element methods.

Remark 5.1. *Although numerical experiments show that convergence order of velocity in L^2-norm for MINI-FVEM is $O(h^2)$, but in the theoretical analysis, we find that the bilinear form of poisson operator in MINI-FVEM does not satisfy the orthogonality condition proposed in* [37]*, and the bilinear form of divergence operator in MINI-FVEM is different from corresponding bilinear form in MINI mixed* *finite element methods. Therefore, we can not give a proof of the error estimate in L^2-norm for velocity of MINI-FVEM.*

6. Concolusion

In this paper, we contructed and analyzed MINI mixed finite volume element methods for Stokes problem on triangular meshes. Both momentum equation and continuity equation are discreted by finite volume element methods. Then we prove the inf-sup conditions of bilinear form for gradient operator and divergence operator. By element analysis methods, the positive definiteness of bilinear form for Laplacian operator is obtained. Furthermore, the convergence analysis is established.

Acknowledgments

This work is partially supported by the National Science Foundation of China (No. 12071177) and the Science Challenge Project (No. TZ2016002).

References

[1] D. N. Arnold, F. Brezzi, and M. Fortin. A stable finite element for the Stokes equations. Calcolo, 21(4):337–344, 1984.

[2] Philippe Blanc, Robert Eymard, and Raphaèle Herbin. An error estimate for finite volume methods for the Stokes equations on equilateral triangular meshes. Numer. Methods Partial Differential Equations, 20(6):907–918, 2004.

[3] Daniele Boffi, Franco Brezzi, and Michel Fortin. Mixed finite element methods and applications, volume 44 of Springer Series in Computational Mathematics. Springer, Heidelberg, 2013.

[4] F. Brezzi. On the existence, uniqueness and approximation of saddle-point problems arising from Lagrangian multipliers. Rev. Française Automat. Informat. Recherche Opérationnelle Sér. Rouge, 8(R-2):129–151, 1974.

[5] Franco Brezzi and Jim Douglas, Jr. Stabilized mixed methods for the Stokes problem. Numer. Math., 53(1-2):225–235, 1988.

[6] Franco Brezzi and Michel Fortin. Mixed and hybrid finite element methods, volume 15 of Springer Series in Computational Mathematics. Springer-Verlag, New York, 1991.

[7] Zhiqiang Cai and Jaeun Ku. The L^2 norm error estimates for the div least-squares method. SIAM J. Numer. Anal., 44(4):1721–1734, 2006.

[8] Carsten Carstensen, Asha K. Dond, Neela Nataraj, and Amiya K. Pani. Three first-order finite volume element methods for Stokes equations under minimal regularity assumptions. SIAM J. Numer. Anal., 56(4):2648–2671, 2018.

[9] Zhongying Chen, Junfeng Wu, and Yuesheng Xu. Higher-order finite volume methods for elliptic boundary value problems. Adv. Comput. Math., 37(2):191–253, 2012.

[10] Zhongying Chen, Yuesheng Xu, and Jiehua Zhang. A second-order hybrid finite volume method for solving the Stokes equation. Appl. Numer. Math., 119:213–224, 2017.

[11] S. H. Chou. Analysis and convergence of a covolume method for the generalized Stokes problem. Math. Comp., 66(217):85–104, 1997.

[12] S. H. Chou and D. Y. Kwak. Analysis and convergence of a MAC-like scheme for the generalized Stokes problem. Numer. Methods Partial Differential Equations, 13(2):147–162, 1997.

[13] S. H. Chou and D. Y. Kwak. A covolume method based on rotated bilinears for the generalized Stokes problem. SIAM J. Numer. Anal., 35(2):494–507, 1998.

[14] Andrea Cioncolini and Daniele Boffi. The MINI mixed finite element for the Stokes problem: an experimental investigation. Comput. Math. Appl., 77(9):2432–2446, 2019.

[15] Ming Cui and Xiu Ye. Unified analysis of finite volume methods for the Stokes equations. SIAM J. Numer. Anal., 48(3):824–839, 2010.

[16] Robert Eymard, Thierry Gallouët, and Raphaèle Herbin. Finite volume methods. In Handbook of numerical analysis, Vol. VII, Handb. Numer. Anal., VII, pages 713–1020. North-Holland, Amsterdam, 2000.

[17] Robert Eymard and Raphaèle Herbin. A cell-centered finite volume scheme on general meshes for the Stokes equations in two space dimensions. C. R. Math. Acad. Sci. Paris, 337(2):125–128, 2003.

[18] Robert Eymard, Raphaèle Herbin, and Jean Claude Latché. On a stabilized colocated finite volume scheme for the Stokes problem. M2AN Math. Model. Numer. Anal., 40(3):501–527, 2006.
[19] Vivette Girault and Pierre-Arnaud Raviart. Finite element methods for Navier-Stokes equations, volume 5 of Springer Series in Computational Mathematics. Springer-Verlag, Berlin, 1986. Theory and algorithms.
[20] Nasserdine Kechkar and David Silvester. Analysis of locally stabilized mixed finite element methods for the Stokes problem. Math. Comp., 58(197):1–10, 1992.
[21] Sarvesh Kumar and Ricardo Ruiz-Baier. Equal order discontinuous finite volume element methods for the Stokes problem. J. Sci. Comput., 65(3):956–978, 2015.
[22] Jian Li and Zhangxin Chen. A new stabilized finite volume method for the stationary Stokes equations. Adv. Comput. Math., 30(2):141–152, 2009.
[23] Jian Li and Zhangxin Chen. On the semi-discrete stabilized finite volume method for the transient Navier-Stokes equations. Adv. Comput. Math., 38(2):281–320, 2013.
[24] Jian Li and Zhangxin Chen. Optimal L^2, H^1 and L^∞ analysis of finite volume methods for the stationary Navier-Stokes equations with large data. Numer. Math., 126(1):75–101, 2014.
[25] Jian Li, Zhangxin Chen, and Yinnian He. A stabilized multi-level method for non-singular finite volume solutions of the stationary 3D Navier-Stokes equations. Numer. Math., 122(2):279–304, 2012.
[26] Jian Li, Xin Zhao, and Zhangxin Chen. A novel L^∞ analysis for finite volume approximations of the Stokes problem. J. Comput. Appl. Math., 279:97–105, 2015.
[27] Ronghua Li, Zhongying Chen, and Wei Wu. Generalized difference methods for differential equations, volume 226 of Monographs and Textbooks in Pure and Applied Mathematics. Marcel Dekker, Inc., New York, 2000. Numerical analysis of finite volume methods.
[28] Xu Li and Hongxing Rui. A low-order divergence-free h(div)-conforming finite element method for stokes flows. IMA J. Numer. Anal., 42(4):3711–3734, 2022.
[29] Yanping Lin, Min Yang, and Qingsong Zou. L^2 error estimates for a class of any order finite volume schemes over quadrilateral meshes. SIAM J. Numer. Anal., 53(4):2009–2029, 2015.
[30] Yanping Lin and Qingsong Zou. Superconvergence analysis of the MAC scheme for the two dimensional Stokes problem. Numer. Methods Partial Differential Equations, 32(6):1647–1666, 2016.
[31] Serge Nicaise and Karim Djadel. Convergence analysis of a finite volume method for the Stokes system using non-conforming arguments. IMA J. Numer. Anal., 25(3):523–548, 2005.
[32] Alfio Quarteroni and Ricardo Ruiz-Baier. Analysis of a finite volume element method for the Stokes problem. Numer. Math., 118(4):737–764, 2011.
[33] Hongxing Rui. Analysis on a finite volume element method for Stokes problems. Acta Math. Appl. Sin. Engl. Ser., 21(3):359–372, 2005.
[34] Hongxing Rui. A conservative characteristic finite volume element method for solution of the advection-diffusion equation. Comput. Methods Appl. Mech. Engrg., 197(45-48):3862–3869, 2008.
[35] Hongxing Rui and Xiaoli Li. Stability and superconvergence of MAC scheme for Stokes equations on nonuniform grids. SIAM J. Numer. Anal., 55(3):1135–1158, 2017.
[36] Wanfu Tian, Liqiu Song, and Yonghai Li. A stabilized equal-order finite volume method for the Stokes equations. J. Comput. Math., 30(6):615–628, 2012.
[37] Xiang Wang and Yonghai Li. L^2 error estimates for high order finite volume methods on triangular meshes. SIAM J. Numer. Anal., 54(5):2729–2749, 2016.
[38] Xiu Ye. On the relationship between finite volume and finite element methods applied to the Stokes equations. Numer. Methods Partial Differential Equations, 17(5):440–453, 2001.
[39] Xiu Ye. A discontinuous finite volume method for the Stokes problems. SIAM J. Numer. Anal., 44(1):183–198, 2006.
[40] Tie Zhang and Zheng Li. A finite volume method for Stokes problems on quadrilateral meshes. Comput. Math. Appl., 77(4):1091–1106, 2019.
[41] Tie Zhang and Lixin Tang. A stabilized finite volume method for Stokes equations using the lowest order $P_1 - P_0$ element pair. Adv. Comput. Math., 41(4):781–798, 2015.
[42] Zhimin Zhang and Qingsong Zou. Vertex-centered finite volume schemes of any order over quadrilateral meshes for elliptic boundary value problems. Numer. Math., 130(2):363–393, 2015.

School of Mathematics, Jilin University, Changchun 130012, Jilin, China
E-mail: `yang_hungtao@163.com and yonghai@jlu.edu.cn`